

# Double Parton Scattering Effects on the Measurement of $W$ -Boson Mass

Rui Zhang<sup>1,\*</sup> and Zhen Zhang<sup>2,†</sup>

<sup>1</sup>*Theoretical Physics Division, Institute of High Energy Physics,  
Chinese Academy of Sciences, Beijing 100049, China*

<sup>2</sup>*Key Laboratory of Particle Astrophysics, Institute of High Energy Physics,  
Chinese Academy of Sciences, Beijing 100049, China*

Double parton scattering (DPS) corresponds to events where two parton-parton scatterings occur in a single hadron-hadron collision. The DPS effects may arise from the spectator scatterings that are somewhat related to soft QCD activities. In this work, we investigate the DPS effects on the  $W$ -boson mass measurements. Especially, our analysis reveals that the DPS events contribute additional missing transverse momenta from spectator scatterings as well as relevant inclusive cross sections, potentially altering the distribution of total missing transverse momenta. Consequently, the DPS effects have the potential to cause an increase in the measured  $W$ -boson mass by the CDF detector, which helps to understand the deviation of the CDF-II measurements from other measurements and the predicted value in the Standard Model.

*Introduction.*— The QCD factorization theorem [1] claims that, for sufficiently inclusive cross sections, the hadron-hadron collision can be factorized into universal parton distribution functions, convoluted with hard parton-parton scattering cross sections. Hence, the hadron-hadron collision can be viewed as a consequence of one parton from each hadron interacting perturbatively. However, it is also possible that more than one parton-parton scattering occurs in a single hadron-hadron collision, which is referred to as multi-parton interactions (MPIs) [2–4]. Although mostly producing low transverse momentum ( $p_T$ ) particles, the MPI can also generate high  $p_T$  particles. The former, combined with beam-beam remnants interactions, is known as the underlying event (UE) [2, 5, 6] activity, which is usually dealt with phenomenological models in the Monte Carlo (MC) event generators [7–9], whereas the later is called double parton scattering (DPS) [10, 11], depicting events where two pairs of partons participate in strong interactions in a single hadron-hadron collision.

In data analyses, the MPI effects are considered in the MC simulation codes through the UE and DPS tunes. Nonetheless, as per the CMS CP5 tune [12], the UE description does not match the experimental data for leading jets with transverse momenta larger than 5 GeV. This suggests the need for the DPS tune when  $p_T$  of leading jets exceeds a threshold of  $p_{T,\text{cut}}^{\text{DPS}} \gtrsim 5$  GeV. Notice that all the thresholds used in experiments are higher than 30 GeV [13]. Ergo, neither the UE nor DPS tune has effectively been used to describe the events with  $p_T^j \sim 5 - 30$  GeV. However, these semi-hard events may have significant influence on measuring inclusive cross sections and missing transverse momenta [14]. Therefore, it is important to find ways to probe the DPS effects in  $\sim 5 - 30$  GeV  $p_T$ -regions, especially at lower intensity colliders like the Tevatron.

Recently, the CDF collaboration reported the latest measurement result of the  $W$  boson mass [15]. The results from the fit of transverse momentum  $p_T^\ell$ , missing

transverse momentum  $p_T^{\text{miss}}$  and transverse mass  $m_T$  of charged leptons  $\ell = e^\pm, \mu^\pm$  are [15]:

$$\begin{aligned} M_W(p_T^\ell(e)) &= 80411.4 \pm 10.7_{\text{stat}} \pm 11.8_{\text{syst}} \text{ MeV}, \\ M_W(p_T^{\text{miss}}(e)) &= 80426.3 \pm 14.5_{\text{stat}} \pm 11.7_{\text{syst}} \text{ MeV}, \\ M_W(m_T(e, \nu)) &= 80429.1 \pm 10.3_{\text{stat}} \pm 8.5_{\text{syst}} \text{ MeV}, \\ M_W(p_T^\ell(\mu)) &= 80428.2 \pm 9.6_{\text{stat}} \pm 10.3_{\text{syst}} \text{ MeV}, \\ M_W(p_T^{\text{miss}}(\mu)) &= 80428.9 \pm 13.1_{\text{stat}} \pm 10.9_{\text{syst}} \text{ MeV}, \\ M_W(m_T(\mu, \nu)) &= 80446.1 \pm 9.2_{\text{stat}} \pm 7.3_{\text{syst}} \text{ MeV}, \end{aligned}$$

where  $m_T \equiv \sqrt{2(p_T^\ell p_T^{\text{miss}} - \vec{p}_T^\ell \cdot \vec{p}_T^{\text{miss}})}$  contains the  $p_T^{\text{miss}}$  information. The results from the  $p_T^{\text{miss}}$  and  $m_T$  fits are systematically higher than the  $p_T^\ell$  fit. With these results from different channels and distributions, they give the combined result

$$M_W = 80433.5 \pm 6.4_{\text{stat}} \pm 6.9_{\text{syst}} \text{ MeV},$$

which is not only  $6.9\sigma$  deviation from the standard model (SM) prediction  $M_W^{\text{SM}} = 80359.1 \pm 5.2$  MeV [16], but also  $3.6\sigma$  deviation from the most precise result of  $M_W = 80366.5 \pm 15.9$  MeV from other measurements [17]. Actually, the ATLAS collaboration also reported a higher  $W$  boson mass in the  $m_T$  fit than the  $p_T^\ell$  fit:

$$\begin{aligned} M_W(p_T^\ell) &= 80362 \pm 16 \text{ MeV}, \\ M_W(m_T) &= 80395 \pm 24 \text{ MeV}. \end{aligned}$$

Indeed, we can find similar discrepancies in different situations; see more details in Fig. 6 of [17].

Given the high level of precision of  $\sim 10^{-4}$  achieved in the CDF-II measurements, the effects that are normally deemed insignificant may no longer be negligibly small, requiring thorough discussion and examination. One significant feature of these measurements is that most of the signal events involve low- $p_T$   $W$  boson production at the Tevatron. So an accurate simulation of the  $W$  boson production associated with soft activities is extremely

important to match the experimental uncertainties. In this work, we will investigate the effects of DPS on measuring the  $W$  boson mass at the Tevatron with detector-level simulations. Conversely, by attributing the  $W$ -mass tension to the DPS effects, we can place further constraints on the DPS threshold.

*The DPS effects.*— The DPS effects can potentially produce additional soft hadrons and alter event distributions in low- $p_T$  regions [18]. As indicated in the CMS data, the production of  $W^\pm W^\pm$  bosons from the DPS processes is already at 6.2 standard deviations, with the DPS effective cross section  $\sigma_{\text{eff}} = 12.2^{+2.9}_{-2.2}$  mb [19]. Measuring the DPS processes has been done in various channels at the LHC [20–31]. Experiments at the Tevatron also offer consistent DPS effective cross section values with the LHC [32–36]. So it is reasonable to set the DPS effective cross section at 12.2 mb, in line with the central value measured at the LHC.

For any single parton scattering (SPS) process, it may suffer from the effects of the DPS process, which can be viewed as a common SPS process and a spectator parton-parton scattering. The spectator scatterings are somewhat associated with soft activities and the resultant radiations can be finally clustered into the final state leptons, jets, and invisible particles. In practical measurements, these final state leptons are generally reconstructed before jets due to their clear backgrounds, so their transverse momenta are rarely affected by the DPS processes. Although the soft radiations may contribute the non-prompt leptons, they are unlikely to change the transverse momenta of the hard leptons from heavy  $W$  boson decays. In addition, the final state jets will be affected little as soft hadrons are already included in the jet clustering. The infrared safety of the jet algorithm guarantees that the clustered jets can be viewed as contributions from two separate parton-parton scatterings. Correspondingly, the total missing transverse momentum can be also calculated by adding the missing transverse momenta from two constituent parton-parton scatterings. In general, the hadron decay, detector response, and other relevant factors contribute a small non-zero residue of total transverse momentum, correspondingly leading to extra contributions from spectator scatterings to missing transverse momenta. These extra contributions, related to the DPS processes, will modify the  $p_T^{\text{miss}}$  and  $m_T$  distributions.

The DPS cross section can be estimated with the product of the two SPS cross sections to produce processes  $S$  and  $P$  independently, as [37, 38]

$$\sigma_{S+P}^{\text{DPS}} = \frac{n}{2} \frac{\sigma_S^{\text{SPS}} \sigma_P^{\text{SPS}}}{\sigma_{\text{eff}}}, \quad (1)$$

where  $\sigma_{\text{eff}}$  is the so-called (universal) effective cross-section,  $n$  is the symmetry factor that equals 1 if  $S = P$ , and 2 otherwise. For example, if the  $S$  process is defined as a process of dijet production, the DPS cross section

reads:

$$\sigma_{jj+X}^{\text{DPS}} = \frac{\sigma_{jj}^{\text{SPS}}}{\sigma_{\text{eff}}} \times \sigma_X^{\text{SPS}},$$

where  $X \neq jj$  is assumed. For a specific SPS process  $P$  ( $\rightarrow X \neq jj$ ), the dijet production process can be viewed as a spectator process, leading to an enhancement of the overall  $\sigma_{jj}^{\text{SPS}}/\sigma_{\text{eff}}$  factor for process  $P$ , seen as a participant process producing  $X$  ( $\neq jj$ ). Note that the MPI can be modeled as the DPS and UE when the jet  $p_T$  is above or below a threshold known as the DPS threshold, respectively. The UE effect is already incorporated in common MC simulation codes to describe the low  $p_T$  events. However, the DPS effects should be taken into account as well. Denoted the DPS threshold as  $p_{T,\text{cut}}^{\text{DPS}}$ . Here, we take  $p_{T,\text{cut}}^{\text{DPS}} = 10$  GeV as an example. Given that  $\sigma_{jj}^{\text{SPS}} \approx 5 \times 10^8$  pb at the 1.96 TeV Tevatron with  $p_T^j > p_{T,\text{cut}}^{\text{DPS}} = 10$  GeV, we obtain  $\sigma_{jj+X}^{\text{DPS}} = 4\% \times \sigma_X^{\text{SPS}}$ . This DPS contribution introduces a  $\sim 4\%$  correction to all the inclusive processes, consequently modifying the  $p_T^{\text{miss}}$  and  $m_T$  distributions. In the following, we could illustrate these modifications by assigning  $X = W^\pm$  for example.

The overall  $\sim 4\%$  factor is calculated using a DPS threshold of  $p_{T,\text{cut}}^{\text{DPS}} = 10$  GeV. In fact, the DPS cross section estimation already sets a lower limit of  $p_{T,\text{cut}}^{\text{DPS}}$ . Generally,  $\sigma_S^{\text{SPS}}$  increases sharply with decreasing  $p_{T,\text{cut}}^{\text{DPS}}$ . In particular, when  $p_{T,\text{cut}}^{\text{DPS}}$  is small enough, the cross section  $\sigma_S^{\text{SPS}}$ , like an inelastic cross section, can even exceed  $\sigma_{\text{eff}}$ ; note, the total inelastic cross section, with a vanishing  $p_T$  cut, is significantly larger than  $\sigma_{\text{eff}}$  [39, 40]. Therefore, Eq. (1) is no longer valid for sufficiently small  $p_{T,\text{cut}}^{\text{DPS}}$ , and hence the corresponding DPS description; otherwise,  $\sigma_{S+P}^{\text{DPS}} \gtrsim \sigma_S^{\text{SPS}}$  or  $\sigma_{S+P}^{\text{DPS}} \gtrsim \sigma_P^{\text{SPS}}$ , which fails to satisfy our statistical expectations. If  $p_{T,\text{cut}}^{\text{DPS}} \sim 10$  GeV, the modification factor of  $\sim 4\%$  closely aligns with the relative uncertainties in the Drell-Yan  $W$  and  $Z$  boson measurements [41–44]. Generally, a decrease in  $p_{T,\text{cut}}^{\text{DPS}}$  leads to a greater modification of the total and differential cross sections. Thus, if  $p_{T,\text{cut}}^{\text{DPS}} \lesssim 10$  GeV, the effects related to the DPS processes should have been detected in these experiments. Actually, no anomalies have been observed in current measurements. Therefore,  $p_{T,\text{cut}}^{\text{DPS}}$  should not be much smaller than 10 GeV. Hereafter, we choose  $p_{T,\text{cut}}^{\text{DPS}} = 10$  GeV as a benchmark point.

Next let us illustrate the DPS effects of the spectator dijet production process on the  $p_T^{\text{miss}}$  distribution of DPS-only events. Specifically, the missing transverse momentum  $p_{T,\text{DPS}}^{\text{miss}}$  from the DPS process can be described as

$$(\vec{p}_{T,\text{DPS}}^{\text{miss}})^2 = (\vec{p}_{T,\text{SPS}}^{\text{miss}})^2 + (\vec{p}_{T,jj}^{\text{miss}})^2 + 2\vec{p}_{T,\text{SPS}}^{\text{miss}} \cdot \vec{p}_{T,jj}^{\text{miss}}, \quad (2)$$

where the subscript “DPS” refers to the DPS process, and “SPS” is used for the SPS process. Roughly,

these DPS effects can be divided into two categories: a smearing effect, broadening the distribution, and a shift effect, hardening the distribution. As shown in Eq. (2), the smearing can be induced by the last term, i.e.,  $2\vec{p}_{T,SPS}^{\text{miss}} \cdot \vec{p}_{T,jj}^{\text{miss}}$ , where  $p_{T,jj}^{\text{miss}}$  denotes the missing transverse momentum generated from the spectator dijet production process. As demonstrated below, the resolution of the smearing can be estimated as  $\langle p_{T,jj}^{\text{miss}} \rangle \sim 4.2$  GeV by simulations, where  $\langle p \rangle$  represents the average of  $p = |\vec{p}|$  over all events for momentum  $\vec{p}$ . Also, the DPS effect can cause a momentum shift in the  $p_T^{\text{miss}}$  distribution. First, we expand  $p_{T,DPS}^{\text{miss}}$  in terms of  $p_{T,jj}^{\text{miss}}$  through Eq. (2), followed by averaging by integration of the opening angle between  $\vec{p}_{T,SPS}^{\text{miss}}$  and  $\vec{p}_{T,jj}^{\text{miss}}$ , and consequently, we find that the shift is  $\langle \Delta p_{T,DPS}^{\text{miss}} \rangle \approx \langle (p_{T,jj}^{\text{miss}})^2 \rangle / (4\langle p_{T,SPS}^{\text{miss}} \rangle) \approx 0.11$  GeV to the order of  $(p_{T,jj}^{\text{miss}})^2$ , where  $\Delta p_{T,DPS}^{\text{miss}} \equiv p_{T,DPS}^{\text{miss}} - p_{T,SPS}^{\text{miss}}$ . Note that the Jacobian peak [45] occurs at around  $\langle p_{T,SPS}^{\text{miss}} \rangle \sim 40$  GeV for the SPS-only process. Therefore, the DPS effects are more likely to manifest their existence as a smearing in the  $p_T^{\text{miss}}$  distribution rather than a shift.

Similarly to the  $p_T^{\text{miss}}$  case, a smearing and shift can also be induced in the  $m_T$  distribution by the DPS effects. Particularly, the transverse mass  $m_T$  from the DPS process can be estimated as

$$(m_{T,DPS})^2 = (m_{T,SPS})^2 + 2p_T^\ell \Delta p_{T,DPS}^{\text{miss}} - 2\vec{p}_T^\ell \cdot \vec{p}_{T,jj}^{\text{miss}}. \quad (3)$$

Expanding  $m_{T,DPS}$  to the second order of  $p_{T,jj}^{\text{miss}}$  yields

$$\begin{aligned} \Delta m_{T,DPS} = & \frac{1}{m_{T,SPS}} \left[ \frac{p_T^\ell}{p_{T,SPS}^{\text{miss}}} \vec{p}_{T,SPS}^{\text{miss}} \cdot \vec{p}_{T,jj}^{\text{miss}} - \vec{p}_T^\ell \cdot \vec{p}_{T,jj}^{\text{miss}} \right] \\ & + \frac{p_T^\ell}{2m_{T,SPS} p_{T,SPS}^{\text{miss}}} \left[ (p_{T,jj}^{\text{miss}})^2 - \frac{(\vec{p}_{T,SPS}^{\text{miss}} \cdot \vec{p}_{T,jj}^{\text{miss}})^2}{(p_{T,SPS}^{\text{miss}})^2} \right] \\ & - \frac{1}{2(m_{T,SPS})^3} \left[ \frac{p_T^\ell}{p_{T,SPS}^{\text{miss}}} \vec{p}_{T,SPS}^{\text{miss}} \cdot \vec{p}_{T,jj}^{\text{miss}} - \vec{p}_T^\ell \cdot \vec{p}_{T,jj}^{\text{miss}} \right]^2, \end{aligned}$$

where  $\Delta m_{T,DPS} \equiv m_{T,DPS} - m_{T,SPS}$ . In this case, the smearing stems from the first term, and the shift arises from the last two terms. In general,  $\vec{p}_{T,SPS}^{\text{miss}} \approx -\vec{p}_T^\ell$  and  $p_T^\ell \approx p_{T,SPS}^{\text{miss}} \approx m_{T,SPS}/2$ . Thus it can be observed that the smearing has a resolution of  $\langle p_{T,jj}^{\text{miss}} \rangle \sim 4.2$  GeV, akin to that in the  $p_T^{\text{miss}}$  case. In contrast, the  $m_T$  shift is approximately zero, i.e.,  $\Delta m_{T,DPS} \approx 0$ , also obtained by integrating the angle out and taking the average. Constrained by  $\langle m_{T,SPS} \rangle \approx 2\langle p_{T,SPS}^{\text{miss}} \rangle$ , the relative correction induced by the smearing to the  $m_T$  distribution is only half as large as that to the  $p_T^{\text{miss}}$  distribution, which can be validated in simulations.

In short, the DPS effects may smear and shift the  $p_T^{\text{miss}}$  and  $m_T$  distributions. These two effects contribute to the measured  $M_W$  value from data fitting in different ways: the shift directly increase the measured value, while the smearing tends to harden the distributions above a given

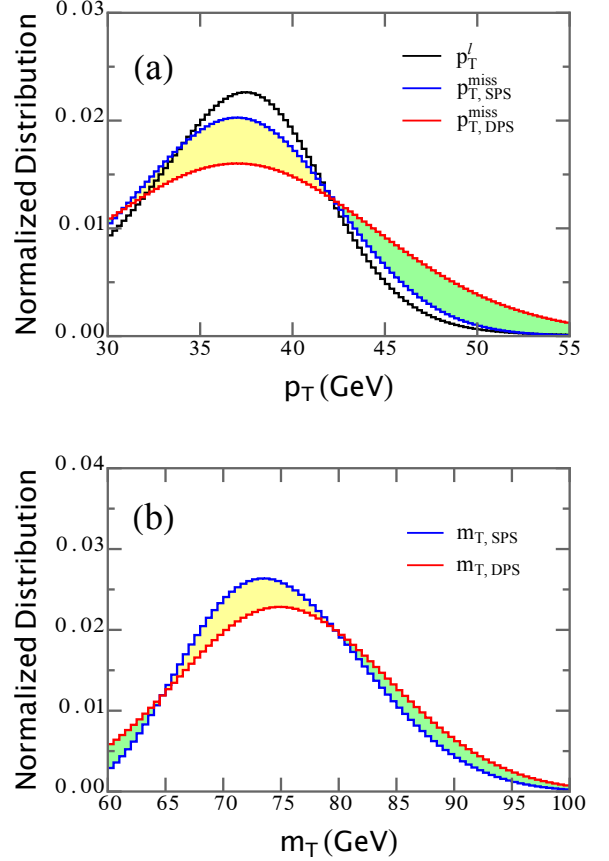


FIG. 1: Normalized distributions for SPS-only and DPS-only contributions. We choose  $p_T^\ell > 10$  GeV for the SPS dijet production process. (a) The black line denotes the  $p_T^{\text{miss}}$  distribution, while blue and red lines represent the  $p_T^{\text{miss}}$  distributions from the SPS and DPS processes, respectively. (b) The blue and red lines represent the SPS and DPS distributions of  $m_T$ , respectively. The yellow and green regions illustrate the differences between the DPS and SPS distributions.

cutoff, such as the  $p_T^{\text{miss}}$  cutoff of  $\sim 30$  GeV and the  $m_T$  cutoff of  $\sim 60$  GeV. Note that compared the smearing, the shift effects are much smaller. Hence, the impact on the fitted  $m_W$  value is primarily attributed to the side effect of smearing, arising from the asymmetry observed in the distributions of  $p_T^{\text{miss}}$  and  $m_T$  over their fitting intervals selected.

In the following analysis, we will focus on the normalized distribution of the signal events from the  $W$  boson production processes. Note that the main background events originate from the  $Z$  boson production processes, only making up  $\sim 7\%$  of all the signal events [15]. Although the distribution of the missing transverse momenta from the background  $Z$  boson production processes may be affected the DPS effects, we neglect the background events from the  $Z$  boson production processes due to their small

contribution to total number of events.

*Simulation and analysis.*— To illustrate the DPS effects, we perform detailed simulations at the 1.96 TeV Tevatron. Overall, we generate 100 million dijet production events using **MadGraph5** [46] at leading order with **CT18NNLO** parton distribution functions [47] at parton level. In particular, we apply the cut  $p_T^j > 10$  GeV at the parton level. Then, we utilize **PYTHIA** [7] for parton shower and hadronization simulation and **Delphes** [48] for detector simulation. Consequently, we obtain  $\sigma_{jj}^{\text{SPS}} = 4.6 \times 10^8$  pb and  $\sigma_{jj}^{\text{SPS}}/\sigma_{\text{eff}} = 3.7\%$ .

We obtain the  $p_{T,jj}^{\text{miss}}$  distribution from the simulated dijet events and extract the  $p_{T,\text{SPS}}^{\text{miss}}$  and  $m_{T,\text{SPS}}$  distributions from the CDF-II data. Then we calculate the distributions of  $p_{T,\text{DPS}}^{\text{miss}}$  and  $m_{T,\text{DPS}}$  for the DPS-only processes; more calculation details are shown in Appendix. In panels (a) and (b) of FIG. 1, we illustrate the normalized distributions of SPS-only and DPS-only events, respectively. In comparison to the SPS distributions, the DPS distributions peak at nearly the same locations, indicating that the shift effect is insignificant, but feature a significant extra smearing effect. After including the smearing effect, the  $p_T^{\text{miss}}$  and  $m_T$  distributions are both hardened a lot compared to those from the SPS-only process, resulting in an obvious increase in events in the high-energy band of  $p_T^{\text{miss}} \sim 43 - 55$  GeV or  $m_T \sim 80 - 100$  GeV. When fitting, we usually limit the range to be above a certain cutoff like  $p_T^{\text{miss}} \sim 30$  GeV or  $m_T \sim 60$  GeV. The increase in the number of high-energy events has increased the fitting weight of data points in that energy range; see Appendix for details. As a result, the fitted  $M_W$  will become larger.

Now we quantitatively estimate the smearing effect. For the  $p_T^{\text{miss}}$  fit, the DPS-only distribution deviates significantly from the SPS-only distribution, with  $\sim 12\%$  of events being moved from the yellow area to the green area, as illustrated in panel (a) of FIG. 1. The yellow area is centered at  $p_T^{\text{miss}} \approx 37$  GeV, and the green area is at  $p_T^{\text{miss}} \approx 47$  GeV. This corresponds to an average increase of  $\sim 1.2$  GeV in  $p_T^{\text{miss}}$ . Here, we estimate the DPS effects solely based on normalized  $p_T^{\text{miss}}$  distributions. Note that the DPS events only constitute  $\sim 3.7\%$  of total events. Consequently, after including all the SPS and DPS events, the average increase in  $p_T^{\text{miss}}$  is  $\sim 44$  MeV. Roughly, one has  $\langle p_T^{\text{miss}} \rangle \sim M_W/2$ . Therefore, we expect a  $W$ -boson mass shift of  $\sim 90$  MeV in the  $p_T$  fit. Also for the  $m_T$  fit,  $\sim 4.4\%$  of events transition from the upper portion of the SPS distribution at  $m_T \sim 72$  GeV to the right wing at  $m_T \sim 88$  GeV, while  $1.7\%$  of events move to the left wing at  $m_T \sim 62$  GeV. Given  $\langle m_T \rangle \sim M_W$ , we finally expect a  $W$ -boson mass shift of  $\sim 25$  MeV in the  $m_T$  fit. The  $W$ -boson mass shift might also be subject to modifications due to the statistic uncertainties and systematic uncertainties in the  $p_T^{\text{miss}}$  and  $m_T$  distributions. Considering all these

factors, including shift, smearing, and uncertainties, we anticipate a mass shift of  $\sim 100$  MeV in the  $p_T^{\text{miss}}$  fit and  $\sim 30$  MeV in the  $m_T$  fit.

In each fit, the number of signal events is the summation of the SPS and DPS events, namely

$$n^{\text{SM}} = n_{\text{SPS}}^{\text{SM}} + n_{\text{DPS}}^{\text{SM}}. \quad (4)$$

The total sample size is rescaled to the sample size of  $n = 4236186$  used by the CDF collaboration. We divide the events into 100 bins with  $p_T^{\text{miss}}$  and 80 bins with  $m_T$ . The  $p_T^{\text{miss}}$  fit is performed in the region with  $32 \text{ GeV} < p_T^{\text{miss}} < 48 \text{ GeV}$ , while the  $m_T$  fit in the region with  $65 \text{ GeV} < m_T < 90 \text{ GeV}$ . Following the CDF collaboration, for a given  $M_W$  value, we use the SPS templates (see Appendix) to fit the  $p_T^{\text{miss}}$  and  $m_T$  distributions of signal events. And the goodness of fit is calculated as

$$\chi^2 = \sum_i \frac{(n_i - n_i^{\text{SM}})^2}{n_i^{\text{SM}} + (f_{\text{syst}} n_i^{\text{SM}})^2}, \quad (5)$$

where  $n_i$  is the event number of the  $i$ -th bin, and  $f_{\text{syst}}$  is adapted to be 10%.

For various DPS thresholds  $p_{T,\text{cut}}^{\text{DPS}}$ , we can apply the previous procedure and obtain the fitted values of  $M_W$ , denoted by  $M_W \equiv M_W^{\text{SM}} + \Delta M_W$ , from the  $p_T^{\text{miss}}$ ,  $p_T^{\text{miss}}$  and  $m_T$  distributions. Then, we can combine the fitting results from the three distributions with a weighted average by assuming that the uncertainty of  $M_W$  in each fit is the same as that of the CDF-II measurement [16]. Accordingly, we can derive the combined values of  $M_W$  or the mass shift  $\Delta M_W$ . As expected,  $\Delta M_W$  will decrease with the increasing threshold  $p_{T,\text{cut}}^{\text{DPS}}$ , due to the decreasing dijet cross section. Actually, the mass shift can be roughly expressed as  $\Delta M_W = 56_{-9}^{+10} \text{ MeV} (p_{T,\text{cut}}^{\text{DPS}}/10 \text{ GeV})^{-3}$ . Here, the uncertainty in  $\Delta M_W$  is derived from that in  $\sigma_{\text{eff}}$ , which is extracted from the CMS same-sign  $W$  boson production measurements [19]. Note that the mass shift  $\Delta M_W$  is rather significant. In fact, even for a large threshold of  $p_{T,\text{cut}}^{\text{DPS}} \sim 20$  GeV, it is already comparable to other higher-order QCD effects, such as the  $N^3\text{LL}+\text{NNLO}$  correction of  $\sim 10$  MeV to the  $W$  mass [49]. In FIG. 2, we depict the scale dependence of  $\Delta M_W$  by the purple line. Correspondingly, we also indicate the increment in the measured  $M_W$  from the CDF-II measurements compared to the SM prediction with a black line, along with its  $1\sigma$  uncertainty calculated by combining the experimental and SPS-related theoretical uncertainties in the  $W$  boson production. The mass shift due to the DPS effects can account for the  $W$ -boson mass discrepancy well, especially in the intersection region indicated by FIG. 2, where the DPS threshold reads  $(9 \pm 1) \text{ GeV}$ .

*Conclusion and discussion.*— In this Letter, we demonstrated the DPS effects on the CDF-II  $W$ -mass measurements and investigated the potential for probing



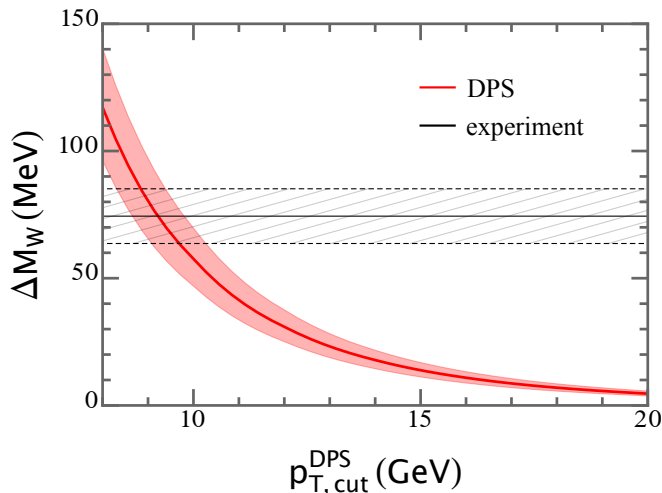


FIG. 2: The mass shift  $\Delta M_W$  as a function of the DPS threshold  $p_{T,\text{cut}}^{\text{DPS}}$ , extracted from the CDF-II data. The red line displays the measured  $W$ -boson mass shift due to the DPS effects. The upper and lower boundaries of the light red region correspond to the values of  $\sigma_{\text{eff}}$  at its  $1\sigma$  lower and upper limits. The region meshed with grey lines indicates the discrepancy between the CDF-II experimental result and the SM prediction. The solid black line stands for the central value, while the dashed ones correspond the  $1\sigma$  bounds, incorporating both experimental and theoretical uncertainties.

these effects through precise  $p_T^{\text{miss}}$  measurements. Note, we tend to focus on the DPS processes with moderate  $p_T$ , as they are expected to have higher production rates and be more sensitive to probe the DPS effects. Particularly in the precise  $W$ -mass measurements, we illustrated that the measured  $M_W$  value can be increased by these DPS effects in both the  $p_T^{\text{miss}}$  and  $m_T$  fits. Specifically, we can combine the fitting results from the  $p_T^\ell$ ,  $p_T^{\text{miss}}$  and  $m_T$  distributions, with the approximation that the uncertainties of  $M_W$  given in each fit are equivalent to those derived from the CDF-II  $W$ -mass measurements, and then obtain the combined  $M_W$  values at different DPS thresholds of  $p_{T,\text{cut}}^{\text{DPS}}$ . Consequently, we can calculate the mass shift  $\Delta M_W$  of the measured  $W$  mass relative to the SM prediction. In fact, this  $M_W$  shift can be generally described as a function of  $p_{T,\text{cut}}^{\text{DPS}}$ , i.e.,  $\Delta M_W \sim 56 \text{ MeV} (p_{T,\text{cut}}^{\text{DPS}}/10 \text{ GeV})^{-3}$ . Clearly, the tension of the measured  $W$  mass by the CDF detector with the SM prediction can be attributed to the DPS effects at a threshold of  $\sim 10 \text{ GeV}$ .

Besides, this mass shift  $\Delta M_W$ , already comparable to the QCD  $\text{N}^3\text{LL}+\text{NNLO}$  correction of  $\sim 10 \text{ MeV}$  to the  $W$  boson mass, has long been overlooked in the  $M_W$  measurements, and hence the closely associated DPS effects. At hadron colliders, the DPS effects associated with soft activities having moderate  $p_T$  cannot be identified directly. To probe these DPS effects and

distinguish them from the other factors such as pile-up and electronic noise, further analyses on the CDF data are necessary. These analyses should focus on addressing soft QCD effects, which may involve extending fitting intervals, varying the cutoffs in the jet algorithm, and improving the jet energy calibration.

Likewise, other precise measurements in processes like the Drell-Yan process may also reveal the sensitivity to investigate the DPS effects. Actually, due to the DPS effects, the total cross section for any inclusive process can be enhanced by  $\sim 10^{-2}$ , and the distribution of missing transverse momenta can also be hardened by  $\mathcal{O}(10^{-2})$  to  $\mathcal{O}(10^{-1}) \text{ GeV}$ . The approaching measurements for rare processes at the LHC, such as the vector boson scattering, di-Higgs production,  $t\bar{t}V$  production, top quark concerned flavor changing neutral current processes, are all affected through enhanced cross sections. Also some precise measurements, like the top quark mass, spin correlation and resonance shape in the  $t\bar{t}$  production process, sensitively depend on performance of missing transverse momentum reconstruction, and may also be influenced by the DPS processes.

We would like to thank Prof. Qing-Hong Cao and Prof. Hao Zhang for useful discussions. This work is supported by the National Program on Key Research and Development Project (Grant No. 2021YFA0718500) from the Ministry of Science and Technology of China, the National Natural Science Foundation of China (Grant Nos. 12273042, 12075257, and 12235001), the Strategic Priority Research Program of the Chinese Academy of Sciences (Grant Nos. XDA15360000, XDA30050000, and XDB0550300), and the funding from the Institute of High Energy Physics (Grant Nos. E25155U1 and Y6515580U1) and the Chinese Academy of Sciences (Grant Nos. E329A3M1, E3545KU2, and Y8291120K2).

\* Electronic address: [rui.z@pku.edu.cn](mailto:rui.z@pku.edu.cn)

† Electronic address: [zhangzhen@ihep.ac.cn](mailto:zhangzhen@ihep.ac.cn)

- [1] J. C. Collins, D. E. Soper, and G. F. Sterman, Adv. Ser. Direct. High Energy Phys. **5**, 1 (1989), hep-ph/0409313.
- [2] T. Sjostrand and M. van Zijl, Phys. Rev. D **36**, 2019 (1987).
- [3] P. V. Landshoff, J. C. Polkinghorne, and D. M. Scott, Phys. Rev. D **12**, 3738 (1975).
- [4] P. V. Landshoff and J. C. Polkinghorne, Phys. Rev. D **18**, 3344 (1978).
- [5] T. Sjostrand, Phys. Lett. B **157**, 321 (1985).
- [6] M. Bengtsson, T. Sjostrand, and M. van Zijl, Z. Phys. C **32**, 67 (1986).
- [7] T. Sjostrand, S. Ask, J. R. Christiansen, R. Corke, N. Desai, P. Ilten, S. Mrenna, S. Prestel, C. O. Rasmussen, and P. Z. Skands, Comput. Phys. Commun. **191**, 159 (2015), 1410.3012.
- [8] M. Bahr et al., Eur. Phys. J. C **58**, 639 (2008), 0803.0883.
- [9] J. Bellm et al., Eur. Phys. J. C **76**, 196 (2016),

- 1512.01178.
- [10] J. R. Gaunt and W. J. Stirling, JHEP **03**, 005 (2010), 0910.4347.
  - [11] J. R. Gaunt, C.-H. Kom, A. Kulesza, and W. J. Stirling, Eur. Phys. J. C **69**, 53 (2010), 1003.3953.
  - [12] A. M. Sirunyan et al. (CMS), Eur. Phys. J. C **80**, 4 (2020), 1903.12179.
  - [13] A. Tumasyan et al. (CMS), JHEP **01**, 177 (2022), 2109.13822.
  - [14] J. Pumplin, Phys. Rev. D **57**, 5787 (1998), hep-ph/9708464.
  - [15] T. Aaltonen et al. (CDF), Science **376**, 170 (2022).
  - [16] J. de Blas, M. Ciuchini, E. Franco, A. Goncalves, S. Mishima, M. Pierini, L. Reina, and L. Silvestrini (2021), 2112.07274.
  - [17] G. Aad et al. (ATLAS) (2024), 2403.15085.
  - [18] C. Goebel, F. Halzen, and D. M. Scott, Phys. Rev. D **22**, 2789 (1980).
  - [19] A. Tumasyan et al. (CMS), Phys. Rev. Lett. **131**, 091803 (2023), 2206.02681.
  - [20] R. Aaij et al. (LHCb), JHEP **06**, 141 (2012), [Addendum: JHEP 03, 108 (2014)], 1205.0975.
  - [21] G. Aad et al. (ATLAS), New J. Phys. **15**, 033038 (2013), 1301.6872.
  - [22] S. Chatrchyan et al. (CMS), JHEP **03**, 032 (2014), 1312.5729.
  - [23] M. Aaboud et al. (ATLAS), Phys. Lett. B **790**, 595 (2019), 1811.11094.
  - [24] R. Aaij et al. (LHCb), JHEP **06**, 047 (2017), [Erratum: JHEP 10, 068 (2017)], 1612.07451.
  - [25] G. Aad et al. (ATLAS), Eur. Phys. J. C **75**, 229 (2015), 1412.6428.
  - [26] R. Aaij et al. (LHCb), JHEP **07**, 052 (2016), 1510.05949.
  - [27] M. Aaboud et al. (ATLAS), JHEP **11**, 110 (2016), 1608.01857.
  - [28] M. Aaboud et al. (ATLAS), Eur. Phys. J. C **77**, 76 (2017), 1612.02950.
  - [29] V. Khachatryan et al. (CMS), JHEP **05**, 013 (2017), 1610.07095.
  - [30] R. Aaij et al. (LHCb), JHEP **08**, 093 (2023), 2305.15580.
  - [31] R. Aaij et al. (LHCb) (2023), 2311.14085.
  - [32] F. Abe et al. (CDF), Phys. Rev. D **47**, 4857 (1993).
  - [33] V. M. Abazov et al. (D0), Phys. Rev. D **89**, 072006 (2014), 1402.1550.
  - [34] V. M. Abazov et al. (D0), Phys. Rev. D **90**, 111101 (2014), 1406.2380.
  - [35] V. M. Abazov et al. (D0), Phys. Rev. Lett. **116**, 082002 (2016), 1511.02428.
  - [36] V. M. Abazov et al. (D0), Phys. Rev. D **93**, 052008 (2016), 1512.05291.
  - [37] B. Humpert and R. Odorico, Phys. Lett. B **154**, 211 (1985).
  - [38] L. Ametller, N. Paver, and D. Treleani, Phys. Lett. B **169**, 289 (1986).
  - [39] A. M. Sirunyan et al. (CMS), JHEP **07**, 161 (2018), 1802.02613.
  - [40] F. Abe et al. (CDF), Phys. Rev. D **50**, 5550 (1994).
  - [41] A. M. Sirunyan et al. (CMS), Phys. Rev. D **102**, 092012 (2020), 2008.04174.
  - [42] S. Chatrchyan et al. (CMS), Phys. Rev. Lett. **112**, 191802 (2014), 1402.0923.
  - [43] M. Aaboud et al. (ATLAS), Eur. Phys. J. C **77**, 367 (2017), 1612.03016.
  - [44] I. Fedorko (CDF) (2006), pp. 193–197.
  - [45] J. Smith, W. L. van Neerven, and J. A. M. Vermaseren, Phys. Rev. Lett. **50**, 1738 (1983).
  - [46] J. Alwall, R. Frederix, S. Frixione, V. Hirschi, F. Maltoni, O. Mattelaer, H. S. Shao, T. Stelzer, P. Torrielli, and M. Zaro, JHEP **07**, 079 (2014), 1405.0301.
  - [47] T.-J. Hou et al. (2019), 1908.11394.
  - [48] J. de Favereau, C. Delaere, P. Demin, A. Giammanco, V. Lemaitre, A. Mertens, and M. Selvaggi (DELPHES 3), JHEP **02**, 057 (2014), 1307.6346.
  - [49] J. Isaacson, Y. Fu, and C. P. Yuan (2022), 2205.02788.

### Appendix: DPS effects and $M_W$ measurements

Here we present the calculation details for the  $p_T^{\text{miss}}$  and  $m_T$  distributions of the signal events from the DPS-only processes. In realistic measurements, as the distributions of  $p_T^\ell$ ,  $p_T^{\text{miss}}$  and  $m_T$  do not show much difference for the electron and muon channels, we do not need to distinguish these two channels. So we simply combine these two channels and obtain the normalized distributions. We extract the  $p_T^\ell$ ,  $p_T^{\text{miss}}$  and  $m_T$  distributions for the  $W$  boson production from the CDF-II data [15]. Then, we can fit these normalized distributions with

$$Z \equiv Z(p; N, x, a, b, c) = \frac{1}{N} \exp \left[ -\frac{(p - xM_W)^2}{(a + b(p - xM_W) + c(p - xM_W)^2)^2} \right], \quad (6)$$

where  $p = p_T^\ell$ ,  $p_T^{\text{miss}}$ ,  $m_T$  for their respective distributions, as well as  $N$ ,  $x$ ,  $a$ ,  $b$ , and  $c$  are five free parameters used for fitting. Generally, one has

$$\begin{aligned} \frac{d\sigma^{\text{SPS}}}{\sigma^{\text{SPS}} dp_T^\ell} &\equiv A(p_T^\ell), \\ \frac{d\sigma^{\text{SPS}}}{\sigma^{\text{SPS}} dp_T^{\text{miss}}} &\equiv B(p_T^{\text{miss}}), \\ \frac{d\sigma^{\text{SPS}}}{\sigma^{\text{SPS}} dm_T} &\equiv C(m_T), \end{aligned} \quad (7)$$

where  $A$ ,  $B$ , and  $C$  can be well fitted into the form of  $Z$  during the data fitting. These equations illustrate how these normalized distributions relate to the cross sections for their respective physical processes. From the fits, we obtain the best-fit values of the parameters, as shown in TABLE I. Here, the  $W$  mass is chosen to align with the SM prediction, i.e.,  $M_W = M_W^{\text{SM}} = 80359.1 \text{ MeV}^1$ . Theoretically, we can adjust the  $M_W$  value in the functions  $Z = A, B, C$  so as to obtain their distributions for any  $M_W$ . These  $Z$  distributions are consistent with those extracted from the best SPS simulations by the CDF collaboration within the experimental uncertainties. Hence, they can serve as templates for describing the SPS processes, also referred as the SPS templates in the main text.

We obtain the  $p_{T,jj}^{\text{miss}}$  distribution of spectator events from the dijet production simulations. This distribution

$$\frac{d\sigma_{jj}}{\sigma_{jj} dp_{T,jj}^{\text{miss}}} = D(p_{T,jj}^{\text{miss}}), \quad (8)$$

<sup>1</sup> Here, for any distribution  $X$ , we first obtain  $s \equiv xM_W^{\text{SM}}$  from data fits. Then in the event analysis, we obtain the best-fit values of  $t \equiv x(M_W^{\text{SM}} + \Delta M_W)$  by fitting the  $p_T^{\text{miss}}$  and  $m_T$  distributions of both SPS and DPS events. Finally, we compute the  $W$  boson mass shift, i.e.,  $\Delta M_W = (t/s - 1)M_W^{\text{SM}}$ , which is insensitive to the  $M_W^{\text{SM}}$  value chosen.

$Z$	$N$	$x$	$a$	$b$	$c$
$A$	11.08	0.4661	6.418	-0.1118	0.01043
$B$	12.34	0.4603	7.880	-0.06364	0.002705
$C$	19.10	0.9145	11.15	0.1256	-0.003254
$D$	8.839	$5.245 \times 10^{-5}$	4.362	0.3924	-0.007343

TABLE I: Best-fit parameters from the experimental results and the simulated dijet events. Each line shows a set of parameters for the distribution in the form of Eq. (6). Note that  $N$ ,  $x$ ,  $a$ ,  $b$ , and  $c$  are in units of GeV, 1, GeV, 1,  $\text{GeV}^{-1}$ , respectively. For  $X = D$ , we choose a cut of  $p_T^j > 10 \text{ GeV}$  for the generated events in the dejet process for example.

can also be well fitted in the same form as Eq. (6), where  $p = p_{T,jj}^{\text{miss}}$ . For example, we apply a cut of  $p_T^j > 10 \text{ GeV}$  on jets at the generator level. In this specific case, we fit the  $p_{T,jj}^{\text{miss}}$  distribution with the function  $D$ , and obtain a set of the best-fit parameters; see TABLE I for details. Note that  $x = 5.245 \times 10^{-5}$  corresponds to  $xM_W = 4.215 \text{ GeV}$ , which is where the peak is located in the  $p_{T,jj}^{\text{miss}}$  distribution.

Let us turn back to the signal  $W$  production processes at the Tevatron. Obviously, the DPS process can be viewed as concurrence of a SPS  $W$  production process, designated as participant process  $P$ , and a SPS dijet process, termed as spectator process  $S$ . Now we can extract the distributions of  $Z = A, B, C$  from process  $P$  by fitting the experimental data and obtain the distribution  $Z = D$  of the events generated in the process  $S$  by simulations using MadGraph5. Thus, we could get the DPS distributions by combining the events from the two SPS processes  $P$  and  $S$ . Clearly, the missing transverse momentum  $p_{T,\text{DPS}}^{\text{miss}}$  from a DPS event can be expressed as

$$p_{T,\text{DPS}}^{\text{miss}} = \sqrt{(p_{T,\text{SPS}}^{\text{miss}})^2 + (p_{T,jj}^{\text{miss}})^2 + 2p_{T,\text{SPS}}^{\text{miss}}p_{T,jj}^{\text{miss}} \cos \alpha},$$

where  $\alpha$  is the open angle between  $\vec{p}_{T,\text{SPS}}^{\text{miss}}$  and  $\vec{p}_{T,jj}^{\text{miss}}$ . Then the  $p_{T,\text{DPS}}^{\text{miss}}$  distribution reads

$$\begin{aligned} \frac{d\sigma^{\text{DPS}}}{\sigma^{\text{DPS}} dp_{T,\text{DPS}}^{\text{miss}}} &= \frac{1}{\pi} \int B(p_{T,\text{SPS}}^{\text{miss}}) dp_{T,\text{SPS}}^{\text{miss}} D(p_{T,jj}^{\text{miss}}) dp_{T,jj}^{\text{miss}} \\ &\times \frac{p_{T,\text{DPS}}^{\text{miss}}}{p_{T,\text{SPS}}^{\text{miss}} p_{T,jj}^{\text{miss}}} \left\{ 1 - \left[ \frac{(p_{T,\text{DPS}}^{\text{miss}})^2 - (p_{T,\text{SPS}}^{\text{miss}})^2 - p_{T,jj}^{\text{miss}2}}{2p_{T,\text{SPS}}^{\text{miss}}p_{T,jj}^{\text{miss}}} \right]^2 \right\}^{-1/2}. \end{aligned}$$

Similarly, the transverse mass  $m_{T,\text{DPS}}$  of a DPS event is:

$$\begin{aligned} (m_{T,\text{DPS}})^2 &= (m_{T,\text{SPS}})^2 + 2p_{T,\text{SPS}}^\ell (p_{T,\text{DPS}}^{\text{miss}} - p_{T,\text{SPS}}^{\text{miss}}) \\ &\quad - 2p_{T,\text{SPS}}^\ell p_{T,jj}^{\text{miss}} \cos \beta, \end{aligned} \quad (9)$$

where  $\beta$  is the open angle between  $\vec{p}_{T,\text{SPS}}^\ell$  and  $\vec{p}_{T,jj}^{\text{miss}}$ . As the spectator processes, such as the dijet production process, are unable to alter the measured transverse momentum  $p_T^\ell$  of electrons or muons,  $p_{T,\text{SPS}}^\ell$  can be

treated the same as  $p_T^\ell$ . Note,  $p_{T,\text{DPS}}^{\text{miss}}$  depends on the angle  $\alpha$ , which is highly correlated with  $\beta$ . In the laboratory frame,  $\vec{p}_{T,\text{SPS}}^\ell$  and  $\vec{p}_{T,\text{SPS}}^{\text{miss}}$  are approximately back to back. Thus, we fix  $\alpha = \pi - \beta$  for simplicity. Additionally, we estimate the joint distributions of  $p_{T,\text{SPS}}^\ell$  and  $p_{T,\text{SPS}}^{\text{miss}}$  from the SPS processes as the product of two independent distributions  $A$  and  $B$ . Accordingly, the  $m_{T,\text{DPS}}$  distributions are calculated as

$$\begin{aligned} & \frac{d\sigma^{\text{DPS}}}{\sigma^{\text{DPS}} dm_{T,\text{DPS}}} \\ &= \int A(p_T^\ell) dp_T^\ell B(p_{T,\text{SPS}}^{\text{miss}}) dp_{T,\text{SPS}}^{\text{miss}} D(p_{T,jj}^{\text{miss}}) dp_{T,jj}^{\text{miss}} \\ & \quad \times \int_0^\pi \frac{d\beta}{\pi} C(m_{T,\text{SPS}}) \frac{m_{T,\text{DPS}}}{m_{T,\text{SPS}}} \bigg|_{m_{T,\text{SPS}}=M_T}, \end{aligned} \quad (10)$$

where  $M_T$  is the solution to  $m_{T,\text{SPS}}$  of Eq. (9):

$$\begin{aligned} M_T^2 &= (m_{T,\text{DPS}})^2 + 2p_{T,\text{SPS}}^\ell p_{T,jj}^{\text{miss}} \cos \beta + 2p_{T,\text{SPS}}^\ell p_{T,\text{SPS}}^{\text{miss}} \\ & \quad - 2p_{T,\text{SPS}}^\ell \sqrt{(p_{T,\text{SPS}}^{\text{miss}})^2 + (p_{T,jj}^{\text{miss}})^2 - 2p_{T,\text{SPS}}^{\text{miss}} p_{T,jj}^{\text{miss}} \cos \beta}. \end{aligned}$$

Following the CDF collaboration, we fit the SPS distributions in the region

$$\begin{aligned} 30 \text{ GeV} &< p_{T,\text{SPS}}^\ell, p_{T,\text{SPS}}^{\text{miss}} < 55 \text{ GeV}, \\ 60 \text{ GeV} &< m_T < 100 \text{ GeV}. \end{aligned}$$

In the calculation, we slightly extend the integral intervals to

$$\begin{aligned} 20 \text{ GeV} &< p_{T,\text{SPS}}^\ell, p_{T,\text{SPS}}^{\text{miss}} < 60 \text{ GeV}, \\ 50 \text{ GeV} &< m_T < 110 \text{ GeV}, \end{aligned}$$

in order to smooth the DPS distributions at their two ends of the fitting intervals.

As already demonstrated in the main text, the DPS effects can alter the  $p_{T,\text{DPS}}^{\text{miss}}$  distribution, thus leading to the changes in the distributions of the measured  $p_T^{\text{miss}}$

and  $m_T$ , as indicated by Eqs. (2) and (3). Note that these changes primarily stem from the smearing, and this DPS effect can alter the fitting results. When we use a SPS template to fit some distribution, the DPS smearing would distort the distribution and change the fitting results. In fact, due to a lack of fully understanding, the quantitative description of the DPS effects has larger uncertainties than those present in the SPS template. Thus, we have to use the SPS template to fit various distributions and measure the  $W$  boson mass. This will induce an apparent  $M_W$  shift to accommodate the ignored DPS effects.

On the other hand, the DPS effects may affect the production processes of  $Z$  bosons as well as  $J/\psi$  and  $\Upsilon$  particles, which are used to calibrate the momenta and energies of the final-state particles like the leptons [15]. However, contrast to the  $W$  boson production, all the final-state particles used in the calibrations are visible. Note that the DPS effects mainly play a role in affecting the detections and measurements of missing transverse energies. Since no missing transverse energies are involved, the calibrations to the observables like  $p_T^\ell$  cannot be changed by the DPS effects. Thus the CDF calibrations do not help to identify the DPS effects.

However, if there is bilateral symmetry in the distribution within the fitting interval selected, the smearing effect on these fitting results will be rather small. For example, if we choose another fitting interval such as  $32 \text{ GeV} < p_T^{\text{miss}} < 42 \text{ GeV}$ , the  $W$  boson mass shift induced by the DPS effects could be reduced. It may be beneficial to only fit distributions over intervals where the distributions are obtained by cutting their high-energy tails off and they become bilaterally symmetric with respect to their peaks, which is far beyond the scope of this work. However, this may lead to a larger uncertainty in the fitted  $M_W$ , and it does not aid in understanding the physics behind the tension observed in the CDF-II  $M_W$  measurement with the SM prediction.